α-Relaxation in the Glass Transition Range of Amorphous Polymers. 1. Temperature Behavior across the Glass Transition

A. Alegría,* E. Guerrica-Echevarría, L. Goitiandía, I. Tellería, and J. Colmenero

Departamento de Física de Materiales, Universidad del País Vasco (UPV/EHU), Facultad de Química, Apartado 1072, 20080 San Sebastián, Spain

ABSTRACT: The effect of the experimental liquid–glass transition on the dielectric relaxation of three amorphous polymers is investigated by means of frequency and time domain dielectric spectroscopies. By means of the time domain experiments, the dynamics of both the supercooled melt and the glassy polymer are characterized. The structural "state" of the glassy polymer is determined by means of differential scanning calorimetry. It is found that the relaxation behavior can be well described by the Kohlrousch–Williams–Watts (KWW) relaxation function above and below T_g. The temperature dependence of the characteristic time scale shows a clear crossover from a Volgel–Fulcher behavior toward an Arrhenius behavior in the liquid–glass transition range. The whole behavior, which extends over 10 decades in time scale, can be fully described by the Adam and Gibbs theory framework, if a slow change of the configurational entropy in the glassy state is allowed. On the other hand, when the system falls out of equilibrium, the KWW shape parameter, β, appears to be slightly higher than the one corresponding to the supercooled liquid. The behavior of β around the glass transition leads us to interpret the relaxation shape as a consequence of a narrow distribution of strongly correlated relaxation processes.

I. Introduction

The dynamics of glass-forming liquids and in particular of polymer melts have been extensively studied during recent years.[1-4] In polymer systems two main dynamical processes are detected by means of mechanical relaxation techniques:[5] (i) the α-relaxation associated with the micro-Brownian motions of main-chain segments and (ii) the terminal relaxation associated with the macroscopic flow. However, by means of other relaxation techniques such as dielectric spectroscopy (DS) or nuclear magnetic resonance (NMR) the α-relaxation is generally the main process observed. Nowadays, it is well established that the α-relaxation shows universal features regardless of the type of glass-forming system considered[1-3] (ionic, low molecular weight organic, inorganic, polymeric, etc.). These characteristic features are (i) the non-Debye behavior observed in the frequency or time dependence of the corresponding susceptibility and (ii) the non-Arrhenius temperature dependence of the characteristic relaxation time. This non-Arrhenius temperature behavior is associated with the strong slowing down of the relaxation rate when the liquid–glass transition is approached from the high-temperature side. The liquid–glass transition phenomenon is commonly characterized by a temperature T_g which, in fact, defines a temperature range where, during cooling, the supercooled melt falls out of the equilibrium-like state and, therefore, a glassy material is obtained. In this temperature range, a nonlinear behavior of the different quantities characterizing the system is universally observed. However, the strong temperature dependence of the characteristic times of the α-relaxation of glass-forming liquids near T_g has led several authors to look for a true thermodynamic transition behind the experimental one.[4,6,7]
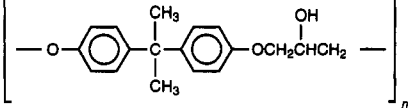
As mentioned above, the liquid–glass transition is related to the loss of the metastable equilibrium of the supercooled melt. Below T_g, a glassy state with very

low mobility is obtained. Two kinds of dynamical processes are observed in the glassy state: the local mobility, evidenced by the presence of secondary relaxation processes,[8] and a very slow dynamics that is evidenced by the so-called structural recovery and physical aging processes.[9,10] It is expected that this slow dynamics should be controlled by the segmental motions in the glassy system which, although having very long characteristic times, are not completely frozen. However, there is only a little experimental information about the behavior of the α-relaxation across the T_g range.[11,12] A reason for this is that, due to the low mobility, any experiment that deals with the dynamics of a glassy system near T_g is very time consuming. As a consequence, during the time of measurement, the structural recovery which is going on will affect to some extent the state of the observed system. This is why most of the investigations on glassy systems close to T_g have focused on observing the time evolution of static properties like volume or enthalpy.[9,13,14]

In this paper, we report on the study of the dynamics around the glass transition of three amorphous polymers, poly(2-hydroxypropyl ether Bisphenol A), poly(vinyl acetate), and poly(vinyl methyl ether). A detailed study of the influence of the physical aging process on the dielectric α-relaxation will be the subject of the second part of this work.[15] Dielectric measurements were performed by using two different experimental setups covering the time range between 10^{-6} and 10^5 s, which includes the time range which is relevant for both the liquid–glass transition and the structural recovery processes in the glassy state close to T_g. Therefore, by means of dielectric techniques we have characterized the time scale and the relaxation shape of the polymers investigated in both the supercooled melt and the glassy state. In addition, enthalpy recovery measurements on the same samples are reported. From these measurements the structural recovery is characterized and an enthalpic recovery time scale extracted. Moreover, by combining both kinds of measurements, we show that, by means of the dielectric time domain method used, it is possible to obtain the dielectric dynamical behavior

Table 1. Main Structural Characteristics of the Polymers Investigated

polymer	T_g (K)	repeating unit	$\overline{M}_n{}^a - \overline{M}_w{}^a$ ($\times 10^3$)	no. of beads[b]
PH	370		$7.68 - 35.54$	6
PVAc	315	$[-CH_2CH-]_n$ OCOCH$_3$	$22.47 - 93.08$	4
PVME	247	$[-CH_2CH-]_n$ OCH$_3$	$18.48 - 112.0$	3

[a] Determined by means of GPC using polystyrene as a reference. [b] Estimated from data of ref 42.

of the glass in a previously determined "state". An interpretation of the results within the framework of the Adams and Gibbs theory[16,17] is outlined.

II. Experimental Section

A. Samples. Poly(2-hydroxypropyl ether Bisphenol A), commonly known as phenoxy (PH), was supplied by Union Carbide (grade PHKK). Poly(vinyl acetate) (PVAc) and poly-(vinyl methyl ether) (PVME) were supplied by Aldrich. The glass transition temperatures of the three polymers were determined from differential scanning calorimetry (DSC) at 10 K/min, after cooling from above T_g at the same rate, from the midpoint of the heat capacity increment. The values of T_g together with other structural characteristics of the three polymers investigated are shown in Table 1.

Samples for dielectric experiments were prepared by melting the "as-received" product directly on the electrodes in a vacuum furnace at T_g + 100 °C. After degassing the sample, the upper electrode was placed on the sample with a light pressure. The sample with the electrodes was maintained under vacuum during the cooling process down to room temperature. Precautions taken during the procedure of the preparation of the samples were similar to those taken in the preparation of the samples for the DSC measurements.

B. Frequency Domain Dielectric Spectroscopy. The dielectric measurements in the frequency domain were performed following standard procedures in the range from 10^{-2} to 10^6 Hz. The experimental setup, which was supplied by Novocontrol GmbH, consisted of a Solarton–Schlumberger frequency response analyzer SI 1260, which was supplemented by using a high-impedance preamplifier of variable gain. The sample was kept between two condenser plates (gold-plated stainless steel electrodes) that were maintained at a fixed distance. Frequency scans were performed at constant temperature, which was decreased in steps. The temperature stability was always better than 0.1 K.

C. Time Domain Dielectric Measurements. The setup used for these measurements consisted of a cylindrical stainless steel cryostat which contained the sample cell. This consists of two aluminum electrodes, isolated by Teflon in the upper part of the cell so the temperature of the Teflon insulator remained constant. The sample (1 mm thick) was placed between the two electrodes to form a parallel-plate capacitor. The temperature of the sample was monitored by a Cerbere temperature controller which provided a temperature stability better than 0.1 K. A Kepco APH 2000 M power supply was used to apply a constant dc voltage of 200 V in order to polarize the sample. The depolarization current was then measured by means of a Keithley 642 electrometer with a resolution of 10^{-17} A.

The followed experimental procedure, which is described in Figure 1, is based on the transient current method,[8] i.e., a box type excitation was applied during a given polarization time t_p, and the corresponding depolarization current was recorded as a function of time.

Two different experiments were performed by this method. First, measurements were performed on well-equilibrated samples, i.e., annealed at the measurement temperature for a time long enough to ensure a depolarization current which does not depend on the previous thermal history. The an-
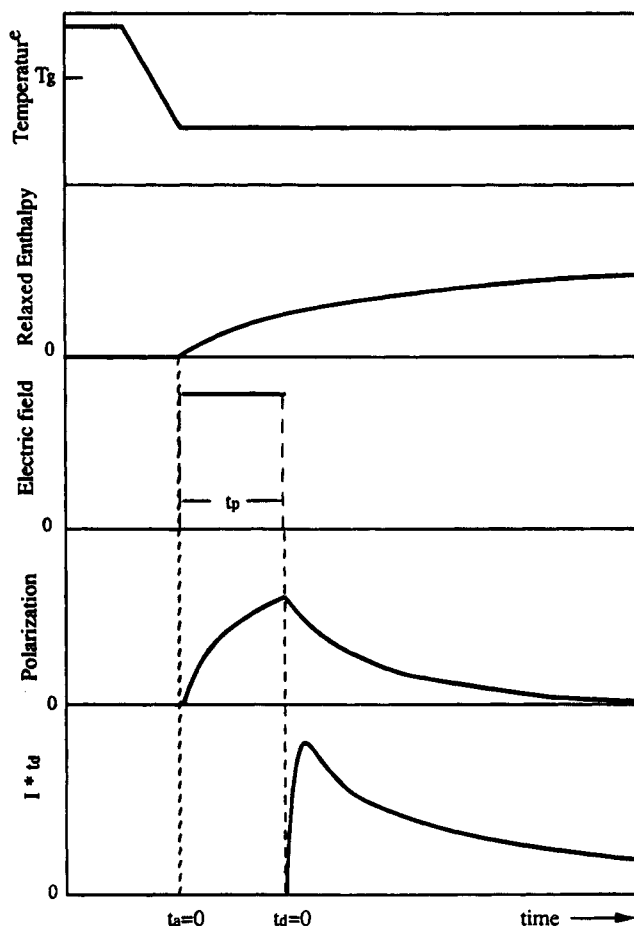

Figure 1. Schematic time evolution of the different quantites involved in the time domain experiments.

nealing time required to obtain this condition was of the same order of magnitude as the one needed to complete the enthalpy relaxation at the same temperature (see below). In a second set of experiments, samples out of equilibrium (in the glassy state) were measured as follows. The sample was first heated up to T_g + 30 K, in order to remove the effects of prior thermal history, and, afterward, cooled at a constant rate (10 K/min) down to the measurement temperature. At this temperature the transient current experiment was immediately started; i.e., the delay between $t_a = 0$ and the time when the polarization field was applied to the sample was just the minimum one necessary to stabilize the temperature. In this way, t_p was close to the annealing time of the sample at the beginning of the depolarization process. Both experimental procedures can be used in the range where the characteristic time of the depolarization process of the sample is greater than the characteristic time of the electrometer response, about 0.1 s, but is small enough to provide measurable values of the depolarization current. These limitations allow us to obtain the dielectric response in the time range from 10^0 to 10^5 s.

In the experiments on nonequilibrated samples, the depolarization current depends on t_p, not only because the degree

of sample polarization depends on it but also because the resulting state of the glassy polymer, and therefore its subsequent depolarization rate, depends on the thermal history. This effect is related to the intrinsic structural instability of the glassy state and will be extensively discussed later.

D. Enthalpy Measurements. A Perkin-Elmer DSC-4 differential scanning calorimeter was used in order to monitor the enthalpy recovery in the $T < T_g$ range. For each scan the temperature was varied at a constant rate of 10 K/min during both the cooling and the heating processes. In order to investigate the enthalpy recovery, isothermal annealing of the samples at several temperatures was performed in the same calorimeter. At the end of each annealing process, the sample was cooled down to below $T_g - 50$ K and the heat capacity $C_p(T)$ was measured during subsequent heating up to $T_g + 30$ K. At this temperature, the effect of the previous thermal history had been totally removed. A consecutive scan on the unannealed sample was immediately performed to serve as a reference. It should be noted that relevant information we will obtain from the DSC experiments refers to the heat capacity differences. Therefore, for this study, the calibration of the DSC enthalpy scale was performed by means of the heat of melting of an indium standard.

The enthalpy recovery during the annealing process was determined by integration of the difference between the two consecutive scans as:

$$\Delta H(T_a, t_a) = \int_{T_a}^{T_g + 20K} [C_p(T', t_a) - C_p(T', 0)] \, dT' \qquad (1)$$

where T_a is the annealing temperature, t_a is the corresponding annealing time, and $C_p(T, 0)$ and $C_p(T, t_a)$ are respectively the specific heats of the unannealed and annealed samples (see Figure 2). The high-temperature limit of the integral in eq 1 is somewhat arbitrary, because it should only be high enough above T_g to ensure the supercooled liquid equilibrium-like state.

III. Results

A. Frequency Domain. The frequency behavior of the dielectric permittivity losses $\epsilon''(\omega)$ for the three samples at several temperatures is shown in Figure 3. As usual, the relaxation was very different from a simple Debye relaxation process.[8,18] The actual relaxation processes are much broader and markedly asymmetric. In addition to this main process, a clear extra contribution to the dielectric losses $\epsilon''(\omega)$ is present at low frequencies and high temperatures, mainly for PH. This contribution, which follows a ω^{-1} law, can be readily attributed to the dc conductivity of the sample, σ_0.

It is well established that the α-relaxation process in glass-forming polymers (and also in low molecular weight systems) can be usually well described by means of a Kohlrausch–Williams–Watts (KWW) relaxation function:[1]

$$\phi(t) = \exp[-(t/\tau)^\beta] \qquad (2)$$

where β is the parameter characterizing the non-Debye nature of the time decay, and τ is a characteristic relaxation time. However, this law gives a description of the relaxation processes which has a closed expression only in the time domain. In the frequency domain the experimental dielectric results have often been described by the Havriliak–Negami (HN)[8,18] empirical relaxation function:

$$\epsilon^*(\omega) = \epsilon_\infty + \Delta\epsilon \frac{1}{[1 + (i\omega\tau_{HN})^\alpha]^\gamma} \qquad (3)$$

where $\epsilon^*(\omega) = \epsilon'(\omega) - i\epsilon''(\omega)$ is the complex permittivity,
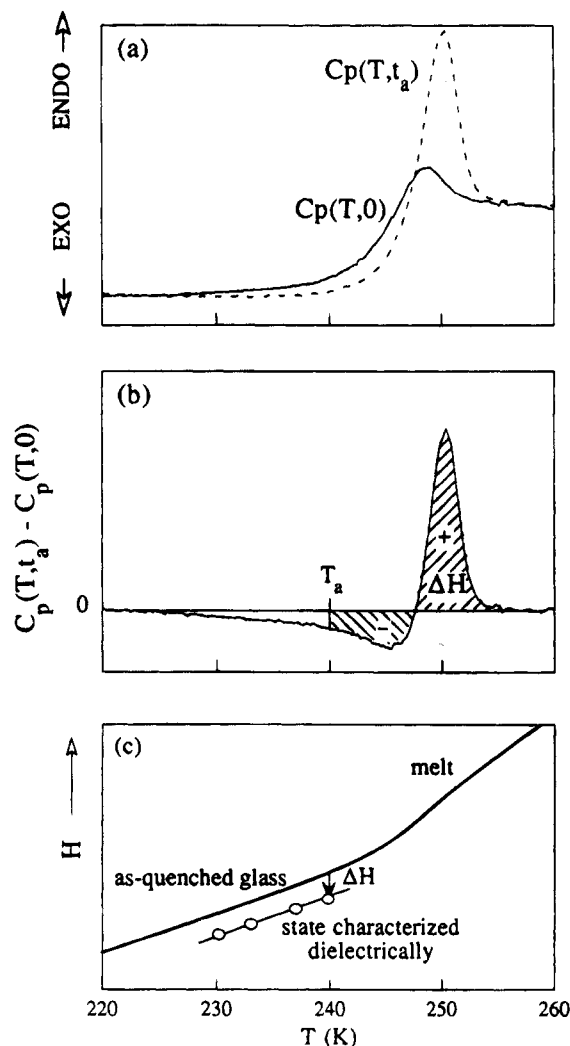

Figure 2. (a) Consecutive DSC scans of PVAc on annealed and nonannealed samples. (b) Schematic plot showing how the relaxed enthalpy is evaluated from the consecutive DSC scans. (c) Schematic temperature variation of the enthalpy throughout the glass transition.

ϵ_∞ is its unrelaxed value, $\Delta\epsilon$ is the relaxation strength, α and γ are two shape parameters in the range zero unity $(0 < \alpha, \gamma < 1)$, and τ_{HN} is a characteristic relaxation time. Since the HN equation has two independent shape parameters, it is more versatile than the KWW one in the sense that the HN equation allows the fitting of the experimental behavior in a wider variety of systems.[8] Furthermore, in eq 3 an extra conductivity term, $-i\sigma_0\omega^{-1}$, is usually introduced to account for the contribution of the conductivity to the dielectric losses.

A comparison between the HN and the KWW descriptions has recently been published.[19,20] In these papers it was shown that, for certain values of α and γ, the HN relaxation function is a good representation of the Fourier transformation (FT) of the KWW time decay function $\phi(t)$. The following empirical correlations among the HN and KWW parameters were reported:[19]

$$\beta = (\alpha\gamma)^{1/1.23} \qquad (4)$$

$$\log \tau = \log \tau_{HN} - 2.6(1 - \beta)^{0.5} \exp(-3\beta) \qquad (5)$$

Moreover, from the obtained results (Table 1 of ref 19) an additional empirical correlation can be deduced between the parameters α and γ corresponding to the
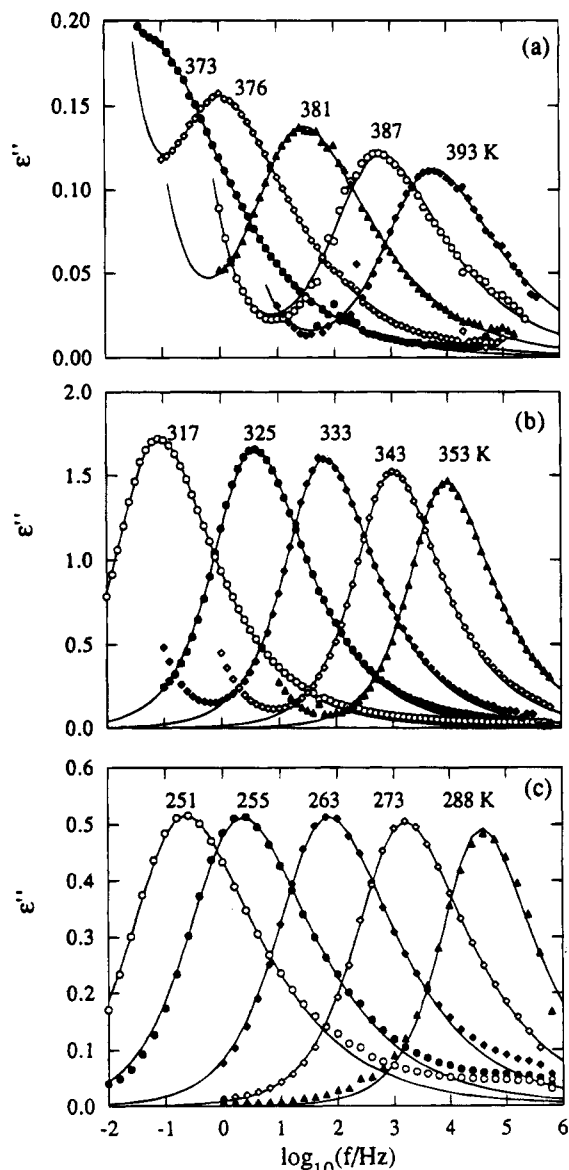
Figure 3. Experimental dielectric losses at several temperatures in the range $T > T_g$ for the three polymers investigated: (a) PH, (b) PVAc, (c) PVME. The lines through the data show the fitting obtained following the method described in the text.

Figure 4. Temperature behavior of the parameters τ and β characterizing the dielectric relaxation above T_g: (a) PH, (b) PVAc, (c) PVME. The lines correspond to fitting curves: Vogel–Fulcher behavior for $\tau(T)$ and straight lines for $\beta(T)$.

HN functions that described the best FT of the KWW behavior:

$$\gamma = 1 - 0.812(1 - \alpha)^{0.387} \qquad (6)$$

Therefore, eqs 3 and 6 allowed us to construct an analytical frequency domain function with a single shape parameter, which to good approximation is the FT of the KWW one. In this work, we have used a least-squares fitting of the experimental $\epsilon''(\omega)$ data by means of eqs 3 and 6 (plus a conductivity term) to obtain the values of the parameters α, τ_{HN}, $\Delta\epsilon$, and σ_0. Solid lines in Figure 3 correspond to the fitting curves thus obtained. Although some deviations in the high-frequency range are apparent, mainly for PVME, which are likely attributed to the contribution of secondary relaxations, the fitting curves describe perfectly the experimental behavior around the α-relaxation loss peak. From the fitting parameters α and τ_{HN}, the KWW parameters τ and β, which we will use to characterize the dynamics of the α-relaxation, were deduced using eqs 4–6. The temperature behavior of these parameters is shown in Figure 4.
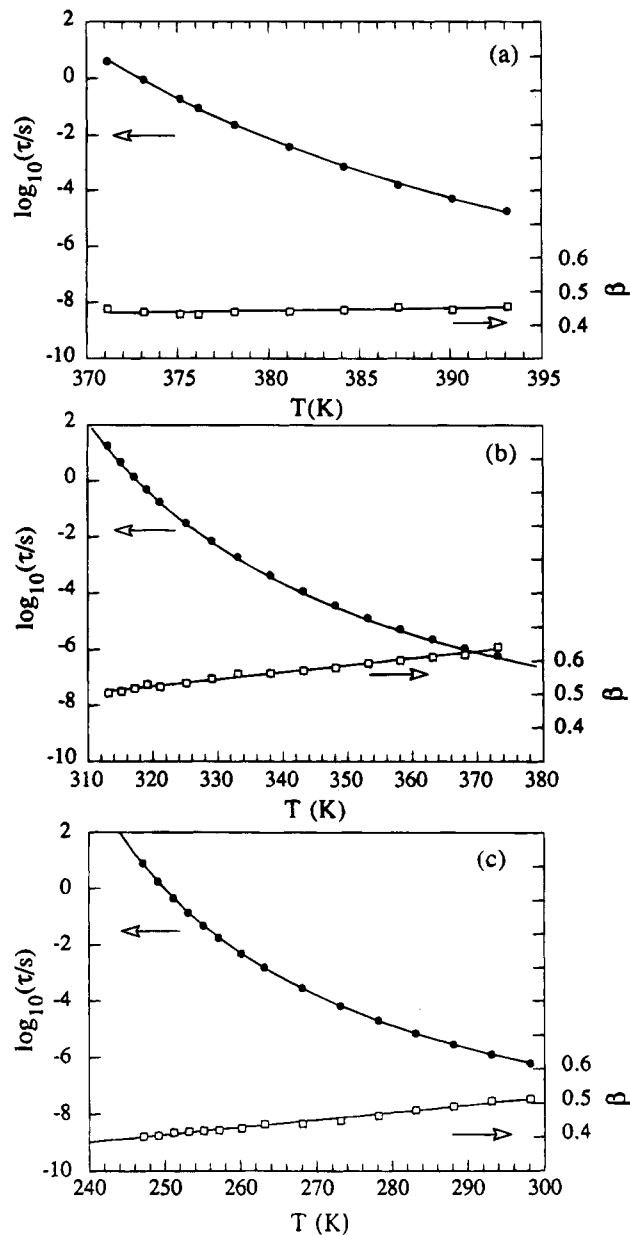
The shape parameter β changes systematically with temperature mainly for PVME and PVAc. Although the behavior obtained for PVAc is in perfect agreement with previous studies,[21-23] at higher temperatures a constant value of β is expected.[22] On the other hand, the change of β with temperature for PVME has not previously been reported in the literature, likely due to the reduced frequency range used in previous studies.[24,25] The obtained $\beta(T)$ behavior, which, in the measuring temperature range, can be approximately represented by a linear increase, is indicated in Table 2.

Concerning the $\tau(T)$ behavior, the usual non-Arrhenius temperature dependence is found. Thus, $\tau(T)$ can be well parametrized by means of the Volgel–Fulcher (VF) equation,

$$\tau(T) = \tau_0 \exp\left(\frac{DT_0}{T - T_0}\right) \qquad (7)$$

Here, T_0 is a temperature below the experimental range

Table 2. Parameters Characterizing the Supercooled Melt Dynamics

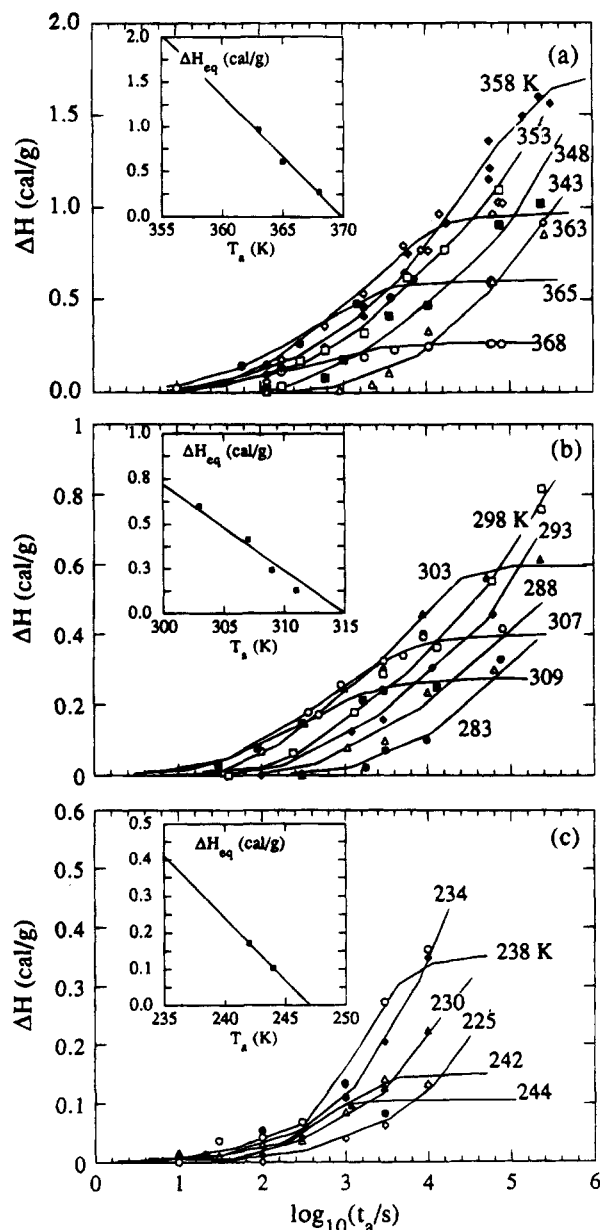| polymer	τ_0 (s)	D	T_0 (K)	$\beta(T)$	$\Delta C_p(T_g)$ (cal g^{-1} K^{-1})	$\Delta\mu$ (kcal mol^{-1})	$\Delta\mu$/bead (kcal mol^{-1})
PH	3.2×10^{-13}	2.76	348	$0.43 \pm 7.7 \times 10^{-4}$ $(T - T_g)$	0.09	13.5	2.2
PVAc	1.0×10^{-12}	5.37	266	$0.51 \pm 2.1 \times 10^{-3}$ $(T - T_g)$	0.11	8.3	2.1
PVME	7.9×10^{-13}	6.03	205	$0.40 + 2.2 \times 10^{-3}$ $(T - T_g)$	0.12	5.5	1.8

Figure 5. Relaxed enthalpy behavior as a function of the annealing time: (a) PH, (b) PVAc, (c) PVME. The lines following the experimental behavior are only a guide for the eye. The insets show the dependence on the annealing temperature, T_a, of the equilibrium relaxed enthalpy [the straight lines correspond to fits according to $\Delta H_{eq} \propto (T_a - T_g)$].

Figure 6. (a) Definition of the enthalpic characteristic times τ_{Heq} and $\tau_{\Delta H}$. (b–d) Temperature dependence of the enthalpic characteristic times for PH, PVAc, and PVME, respectively. ($\times$) τ_{Heq} values, $\tau_{\Delta H}$ for ($\bigcirc$) $\Delta H = 0.1$ cal/g, ($\blacktriangle$) $\Delta H = 0.2$ cal/g, and ($\blacklozenge$) $\Delta H = 0.3$ cal/g. The solid straight lines and curves stand respectively for Arrhenius fits and for the extrapolation of the VF law accounting for the dielectric relaxation time.

at which the extrapolated relaxation time diverges, D is a parameter which can be related to the fragility concept first introduced by Angell,[26] and τ_0, which might depend slightly on temperature, is the reciprocal of an attempt frequency. Solid lines through $\tau(T)$ data in Figure 4 represent VF fits. The values of the VF parameters obtained are shown in Table 2.

B. Enthalpy Recovery. Figure 5 shows the annealing time dependence of the relaxed enthalpy $\Delta H(T_a, t_a)$ at different temperatures for PH, PVME, and PVAc which, as described above, were calculated by means of eq 1. Lines through the data in Figure 5
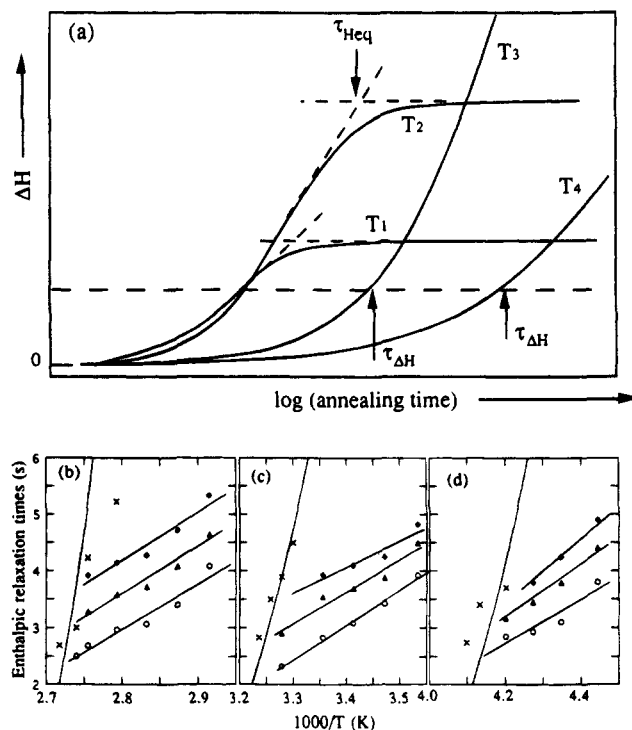
correspond to smooth curves describing the experimental behavior and should be taken only as a guide for the eye.

Due to the nonlinearities inherent to the glassy dynamics, the experimental ΔH behavior shown in Figure 5 cannot be described by means of simple functions like the KWW one. This makes it difficult to obtain information about the glassy dynamics from those data. In spite of this difficulty, in this work, we have tried to use the $\Delta H(t_a)$ behavior to obtain an estimate of the time scale of the enthalpy recovery process. A first estimate of the annealing time required to reach the equilibrium value, τ_{Heq}, has been obtained as indicated in Figure 6a. Although this procedure does not yield rigorous values of the characteristic enthalpy relaxation time, it provides an order of magnitude of it. The values obtained in this way are shown in Figure 6b–d. It is apparent that, within the errors involved, τ_{Heq} conforms to the VF law deduced above from the frequency domain dielectric relaxation times. This agreement could be interpreted as a consequence of the strong correlation between the dielectric and the structural relaxations, which indeed has been evidenced in the study of the influence of physical aging on the dielectric α-relaxation behavior.[15,27,28] However, the fact that the τ_{Heq} values can only be considered as rough estimates makes it difficult to obtain a definitive conclusion from this result.

On the other hand, a different time scale has been evaluated from the annealing time needed at each

Table 3. Parameters Characterizing the Segmental Dynamics in the Glassy State

polymer	ΔH (cal g^{-1})	$\tau_{\infty\Delta H}$ (s)	$\varepsilon_{\Delta H}$ (kcal mol^{-1})	$\beta(T_g)$	$\tau_{\infty D}$ (s)	E_D (kcal mol^{-1})
PH	0.18	2×10^{-19}	37	0.53	1×10^{-22}	44
PVAc	0.20	2×10^{-16}	25	0.54	2×10^{-31}	46
PVME	0.05	1×10^{-17}	22	0.51	2×10^{-23}	30

temperature to obtain a constant value of ΔH (see Figure 6). The menaing of such a time is also not clear. However, one can imagine that, at any time, while the system is evolving toward equilibrium, the characteristic time of the system cannot be much shorter or much larger than the annealing time. In the former case, the system would relax easily to the state where the characteristic time of the system is comparable to the annealing time; in the latter, the system would not been able to start relaxing until the annealing time would be comparable to the characteristic time. Therefore, in the time range where ΔH is far enough from both zero and the equilibrium value, the so-defined $\tau_{\Delta H}$ can be taken to be an estimate of the instantaneous characteristic enthalpic relaxation time of the glass.

The characteristic times $\tau_{\Delta H}(T)$ obtained in this way for three fixed ΔH values (0.1, 0.2, and 0.3 cal/g) are shown in Figure 6b–d. Although the high uncertainty in the ΔH experimental data produces quite scattered values of $\tau_{\Delta H}$, the points corresponding to constant values of ΔH seem to follow approximately Arrhenius-like behaviors:

$$\tau = \tau_\infty \exp(E/k_B T) \qquad (8)$$

τ_∞ being a prefactor, E an apparent activation energy, and k_B Boltzmann's constant. From that behavior it is difficult to see a clear influence of the ΔH value considered on the apparent activation energy, $E_{\Delta H}$. Average values of the prefactor, $\tau_{\infty\Delta H}$, and the apparent activation energy, $E_{\Delta H}$, are shown in Table 3 and will be discused together with the dielectric results.

C. Time Domain Dielectric Measurements. As mentioned above, two different types of dielectric measurements in the time domain have been done. In this section we shall present the results obtained in both cases.

C.1. Equilibrium-like Behavior. In the experimental conditions of our time domain experiments, the isothermal depolarization current can be expressed as the first derivative of the response corresponding to a block shape excitation:[18]

$$I(t) \propto -\frac{d}{dt}[\phi(t) - \phi(t+t_p)] \qquad (9)$$

where $\phi(t)$ is the relaxation decay function corresponding to a fully polarized sample, and $I(t)$ is the depolarization current.

The α-relaxation dynamics in the time domain has also been analyzed by assuming a KWW function for the $\phi(t)$ decay. By fitting the experimental $I(t)$ behavior by means of eqs 2 and 9, the values of τ and β characterizing the dynamics of the dielectric α relaxation were deduced. In Figure 8a, the solid lines are examples of such a fit. The values of τ and β corresponding to PH, PVME, and PVAc in the equilibrium-like state are shown in Figure 7. It must be outlined that, for the data fitting corresponding to PH, a single-exponential decay has been added to eq 9 in order to
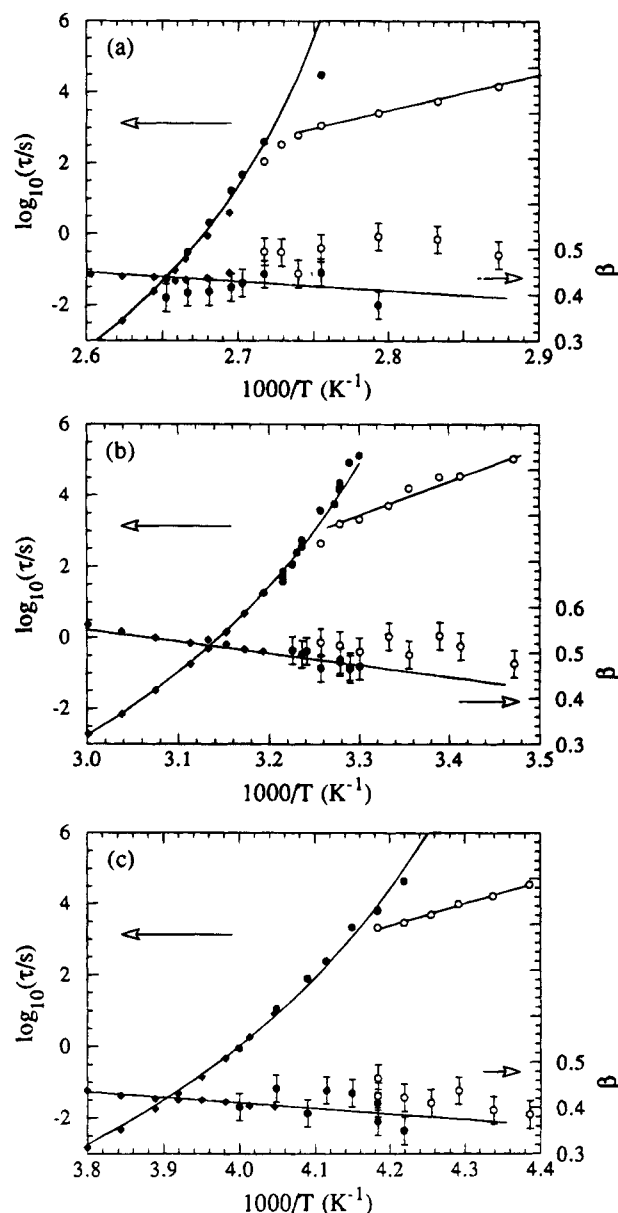

Figure 7. Temperature dependence across the glass transition range of the β and τ parameters characterizing the dielectric dynamics. The filled symbols correspond to the supercooled melt (the diamonds for frequency domain and the circles for time domain) and the open ones to the glassy state. The solid lines stand for VF and Arrhenius fits.

take into account the extra current appearing at the largest times (see Figure 8a). This is likely attributed to the conductivity contribution detected in the frequency domain experiments. This component limits the time range accessible for this polymer and introduces a larger uncertainty in the τ values obtained.

As we can see in Figure 7, the τ values come close to the extrapolation of the VF fitting curves obtained from data in the frequency domain. However, in the lowest temperature range, small deviations are observed. These deviations are more pronounced for PH, likely because the largest errors involved in this polymer related to the important conductivity contributions.

Concerning the β parameter, from the data shown in Figure 7, it is clear that the errors involved using the time domain techniques are higher than those obtained by means of frequency domain experiments. However, within the experimental uncertainty, the values deduced by the time domain methods are in agreement
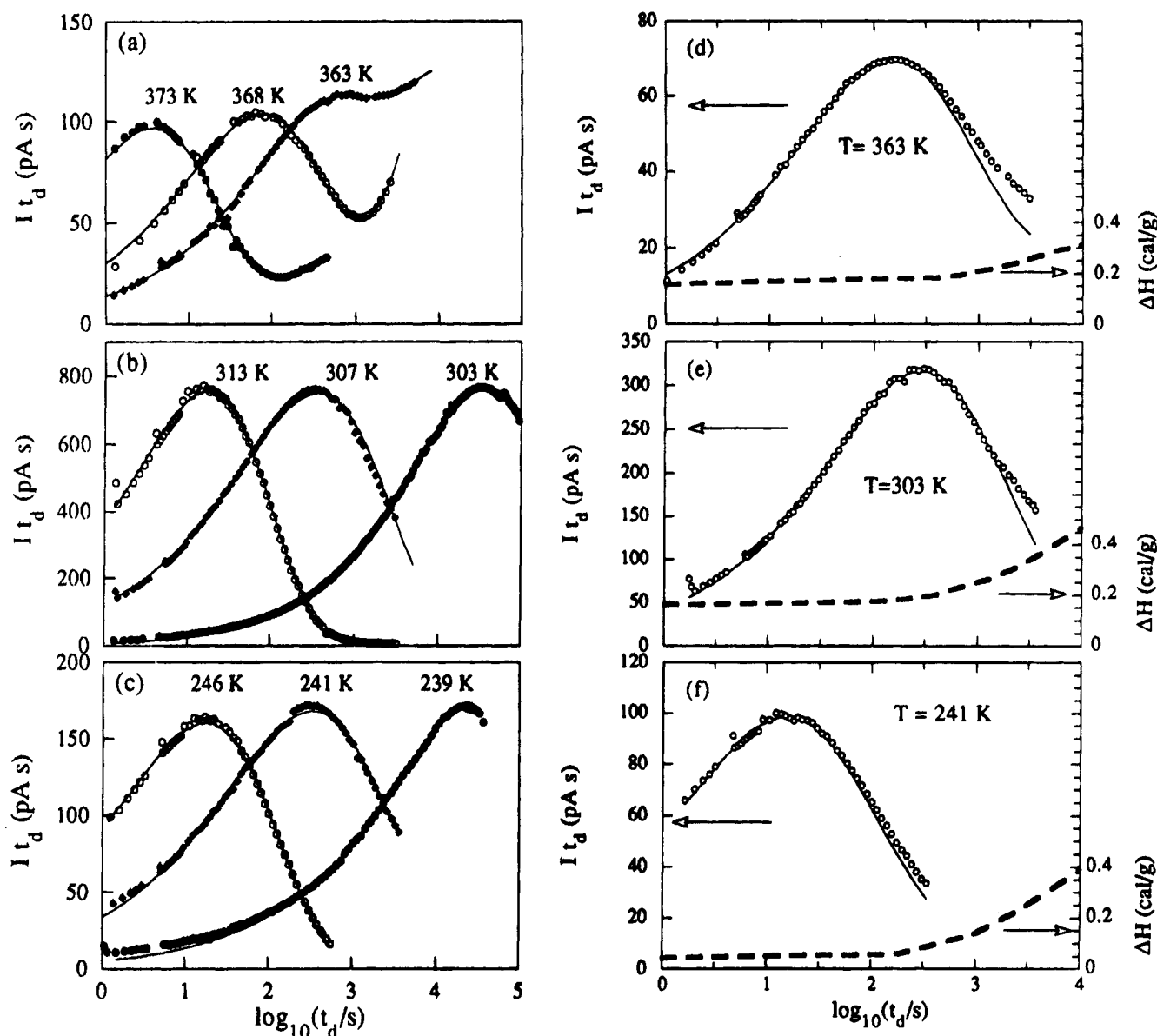
Figure 8. Representative experimental results obtained by means of time domain dielectric measurements both on equilibrated samples PH (a), PVAc (b), and PVME (c) and on nonequilibrated samples PH (d), PVAc (e), and PVME (f). The dashed thick lines represent the evolution of ΔH during the depolarization current measurements. The solid lines stand for KWW fits.

with the temperature dependence obtained from the frequency domain measurements.

C.2. Nonequilibrium Behavior. As mentioned above, in these measurements the sample was cooled from above T_g at a constant rate of 10 K/min down to the temperature of measurement. Then, the electric field was applied during a polarization time t_p, and, after removing the field, the depolarization current was measured as a function of time. By using this procedure, which is schematically described in Figure 1, the dielectric response depends on the measurement conditions because we are dealing with a system that is out of the thermodynamic equilibrium in the sense that the properties (enthalpy, for example) are changing during the experimental time (see Figure 1). Therefore, we have to find out a way of characterizing the dielectric relaxation of the sample in the glassy state as accurately as possible. Two different problems appear in the nonequilibrium measurements. First, how to characterize the instantaneous state of a system when it is evolving during the experiment. Second, if this problem is solved, how to compare the results obtained in the same material at different temperatures. Concerning

the former of these problems, we have tested that, during the initial stages of the depolarization process, the evolution of the sample state is neglectful. This is illustrated in Figure 8d−f where the measured current and the relaxed enthalpy (obtained from data of Figure 5) are plotted as a function of the logarithm of the depolarization time t_d. From this comparison it is apparent that the enthalpy of the sample remains nearly constant during the first part of the depolarization process, namely, until the product It_d passes through a maximum. In addition, the depolarization current behavior during this time range can be well described by assuming a KWW law for $\phi(t)$ (see Figure 8d−f). Thus, also in the glassy state, the dynamics of the system can be characterized by means of the parameters τ and β previously used to characterize the dynamics of the supercooled melt. This is a general property of the experimental procedure here described.

Once this point is clarified, we need to design the experiments in such a way that the results obtained at different temperatures are comparable. First of all, it should be remembered that our experimental method is not able to characterize the response of the glass in

the initial state (immediately after cooling) but when the enthalpy has relaxed in an amount which depends on the experimental details. From the calorimetric study reported above, it is possible to determine the annealing time required at each temperature to obtain a given value of the relaxed enthalpy. Thus, by taking the value of this annealing time to be the time we wait before the depolarization starts at each temperature, the relaxed enthalpy of the sample at the beginning of the depolarization process (the same time range considered in the fitting procedure) will be the same for all temperatures. Therefore, by combining both the experimental method described above and the fitting by means of eqs 2 and 9 of the experimental response up to the maximum of It_d, the values of $\tau(T)$ and $\beta(T)$ corresponding to a glassy state with a constant enthalpy difference from the initial one (obtained after cooling the melt at 10 K/min) are obtained.

The $\tau(T)$ and $\beta(T)$ behaviors obtained by following this procedure are shown in Figure 7. $\tau(T)$ in the glassy state shows an Arrhenius-like behavior (fitting parameters $\tau_{\infty D}$ and E_D are shown in Table 3). The obtained activation energy E_D is systematically higher than the one deduced from the enthalpic results $E_{\Delta H}$. This discrepancy can be attributed to the rather unclear meaning of the enthalpic relaxation times defined above. From inspection of Figure 6b–d, one can realize that the low-temperature data points indicate an activation energy higher than the one corresponding to the lines. A reason for that could be that, at temperatures close to T_g, relaxation occurs during the cooling from T_a, both in the annealed sample and, mostly, in the unannealed sample used as a reference. In fact, the value of E_D obtained for PVAc is not far from the value of the apparent activation energy deduced from calorimetric measurements for this polymer (58 kcal mol^{-1}).[23] Therefore, the values obtained by us from DSC measurements should be considered to be only rough estimates of the actual ones.

Concerning $\beta(T)$, we found that, near T_g, the values obtained in the glassy state are higher than the values deduced from $\beta(T)$ in the supercooled melt (at equilibrium). However, the difference, although systematic, is barely bigger than the estimated uncertainty in β. On the other hand, at lower temperatures, β seems to decrease as the temperature does.

IV. Discussion

Since we have characterized the dynamics of the dielectric α relaxation by means of the time scale τ and the shape parameter β, in this section we will discuss the temperature behavior of these parameters in both the supercooled melt and the glassy state.

A. Temperature Dependence of τ. From the data of Figure 7, it is apparent that the experimental values of $\tau(T)$ obtained at equilibrium by means of the time domain measurements conform approximately to the VF law deduced by fitting the frequency domain ones. However, small deviations are observed at low temperatures. Several modifications of the VF equation have been proposed in the literature on the basis of different models to account for deviations of the $\tau(T)$ behavior from the VF law near T_g.[29,30] However, due to the fact that the deviations we observe are not far apart from the experimental uncertainty, we have preferred not to introduce additional parameters in the fitting procedure and to assume that the VF equation remains valid as a good description of the equilibrium $\tau(T)$ behavior near T_g.

Several theoretical approaches have been used to account for the VF equation, the most popular two being the free volume and the Adams and Gibbs (AG) theories. The free volume model was introduced by Doolittle[31] and further developed by Cohen and Turnbull and Cohen and Grest.[29,32] Although the free volume is a very intuitive concept, its definition is ambiguous and, in fact, different authors have proposed different definitions.[33,34] On the other hand, in the AG theory[16] the main magnitude controlling the dynamics is the configurational entropy. The configurational entropy concept is not as intuitive as the free volume one, but it has a much clearer operational definition (see below). Although both descriptions are possible, in what follows we will discuss the $\tau(T)$ behavior in terms of the AG approach. Now, we briefly summarize the main ideas of this model.

The central assumption of the AG theory is that the molecular dynamics in the supercooled liquid is controlled by cooperative rearrangements of the particles in different regions. In this theory, the number of particles that cooperatively rearrange is assumed to increase with decreasing temperature. It is also assumed that the observed activation energy is the product of the number of particles involved in the cooperative rearrangement and an elemental energy corresponding to the activation energy per particle. Thus, the theoretical expression for the relaxation time in a region with z molecules is written as:

$$\tau = \tau_0 \exp(z\Delta\mu/k_B T) \qquad (10)$$

where $\Delta\mu$ is the elementary activation energy which is independent of the number of rearranging particles, z. It is also assumed that only the minimum value of z, z^*, contributes to the relaxation time. The temperature dependence of z^* is expressed in terms of the configurational entropy as:

$$z^*(T) = N_A s_c^*/S_c(T) \qquad (11)$$

where N_A is Avogadro's number, s_c^* is the entropy of the minimum number of particles able to rearrange, and $S_c(T)$ is the macroscopic configurational entropy per mol of particles. Thus, from eqs 10 and 11 the relaxation time can be written as a function of the configurational entropy as

$$\tau = \tau_0 \exp\left(\frac{N_A s_c^* \Delta\mu}{k_B T S_c(T)}\right) \qquad (12)$$

The final step is to determine the temperature dependence of $S_c(T)$, which is defined as:

$$S_c(T) = \int_{T_0}^{T} \frac{\Delta C_p}{T'} \, dT' \qquad (13)$$

where ΔC_p is the configurational heat capacity and T_0 is the temperature at which S_c extrapolates to 0 (configurational ground-state temperature). Following Angell's approach,[35] the $\Delta C_p(T)$ behavior in the supercooled melt can be considered to be proportional to $1/T$, which is the simplest expression of the experimental observation that ΔC_p decreases with increasing temperature. Thus, taking $\Delta C_p(T) = \Delta C_p(T_g) T_g/T$, from eq 13 we obtain

$$S_c(T) = T_g \Delta C_p(T_g) \frac{T - T_0}{TT_0} \qquad (14)$$

With this expression of $S_c(T)$ eq 12 reduces to:

$$\tau = \tau_0 \exp\left(\frac{N_A s_c^* \Delta\mu T_0}{T_g \Delta C_p(T_g) k_B (T - T_0)}\right) \qquad (15)$$

which has the same form that the VF formula if $D = N_A s_c^* \Delta\mu/T_g \Delta C_p(T_g) k_B$ (see eq 7). It is noteworthy to point out that the heat capacity discontinuity has both vibrational and configurational contributions.[36] For polymers, these vibrational contributions to the experimental measured increment can be estimated to be about 20% of the total increment.[37] However, from the heat capacity increment at the glass transition, as measured in a DSC scan, an experimental estimate of $\Delta C_p(T_g)$ can be extracted regardless of the possible vibrational contributions. Once $\Delta C_p(T_g)$ is evaluated (see Table 2), the values of $\Delta\mu$ can be derived from the values of D obtained above, provided a value of s_c^* is assumed. Although several expressions of s_c^* have been proposed, it has been recently suggested[38] that for polymers a value of $s_c^* = k_B \ln 3!$ is adequate. This value is estimated by taking into account that three chain segments are involved in the crankshaft motions which are reasonable candidates for the localized rearrangements involving the smallest number of chain segments. The values of $\Delta\mu$ obtained in this way are shown in Table 2. In spite of the uncertainties pointed out above, $\Delta\mu$ clearly depends on the considered polymer, being highest for PH which has the largest repeating unit. The values obtained are between 2 and 4 times the energy barrier corresponding to a rotation around a C–C bond (3.1–3.5 kcal/mol)[39] which seems to be reasonable considering the structure of the polymers investigated (see Table 1). Nowadays, it is clear that the fundamental unit driving the segmental dynamics in a polymeric chain is not the repeating unit. Various entities have been introduced to play this role, the more used two being the "bead",[40] defined as the smallest molecular unit which movements may change the whole equilibrium, and the "conformer"[41] defined as the smallest unit able to perform a rotation. In Table 2 we show the values of $\Delta\mu$ calculated per bead. The number of beads of the polymer investigated, which were estimated from ref 42, are shown in Table 1. The values obtained for $\Delta\mu$/bead are similar for the three polymers, although slightly smaller than the energy barrier corresponding to a rotation around a C–C bond.

A series of recent papers has shown that the AG formulation is appropriate to describe the effects of the annealing and prior history on the enthalpy relaxation of glassy polymers;[13,38,43,44] i.e., the AG theory seems also appropriate to describe the relaxational dynamics in the glassy state. On the other hand, one of the main advantages of the AG formalism, when compared with the free-volume one, is that eq 12 gives qualitative account of the Arrhenius-like behavior in the glassy state. In fact, if $S_c(T)$ is assumed to be constant in the glassy state, eq 12 leads directly to an Arrhenius behavior with apparent activation energy $N_A s_c^* \Delta\mu/S_c$. However, as commented on above, the value expected (and obtained above T_g) for the prefactor of eq 12 is $\tau_0 \approx 10^{-12}$ s, which is several orders of magnitude higher than the values of τ_∞ deduced above from the fitting of the experimental $\tau(T)$ in the glassy state by means of an Arrhenius-like law (see Table 3). This fact could
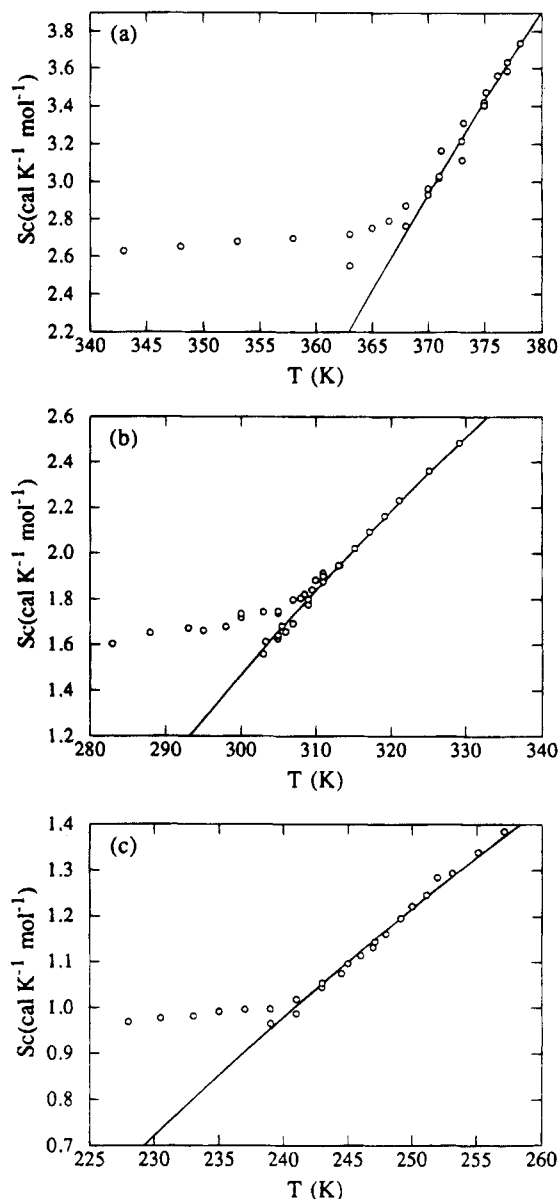

Figure 9. Temperature behavior of the configurational entropy deduced from the dielectric experiments on the basis of the AG theory. The solid lines correspond to eq 14.

indicate that the configurational entropy is not actually constant in the glassy state dielectrically characterized. Although any temperature dependence of $S_c(T)$ would produce a failure of the Arrhenius behavior in the glassy state, the experimental uncertainties allow one to fit the data approximately by means of the Arrhenius law.

An alternative way to proceed is to evaluate $S_c(T)$ without previous assumptions on its behavior in the glassy state. Following this idea and according to eq 12, $S_c(T)$ was calculated from the $\tau(T)$ experimental values as:

$$S_c(T) = \frac{N_A s_c^* \Delta\mu}{k_B T \ln \dfrac{\tau(T)}{\tau_0}} \qquad (16)$$

where τ_0 was taken from the prefactors of the VF formulas shown in Table 2. The results obtained are shown in Figure 9. There, it is apparent that the $S_c(T)$ in the glassy state is not a constant but diminishes slowly with decreasing temperature. This variation of the configurational entropy in the glassy state should

be directly connected with the existence of configurational degrees of freedom in the glass, which could be, in principle, attributed to the presence of secondary relaxation processes. However, the β relaxation of the polymers investigated is located 100 K below T_g which seems to be too far to influence significantly the main characteristics of the segmental dynamics at T_g. Moreover, as is shown in Figure 2a, the change of the heat capacity of a glassy sample as detected in a DSC experiment starts at temperatures well below T_g (see Figure 2), i.e., in the temperature range we have dielectrically characterized. This would indicate that, due to the residual segmental mobility of the glassy state, the configurational entropy is still changing several degrees below T_g and would only raise its constant value below the lower limit ($T_g - 30$ K) of the temperature range we have covered dielectrically. Taking this result into account, it could be considered that the actual glassy polymers below, but relatively close to, T_g cannot be considered to be in a totally frozen state.

The characterization of the state corresponding to a glassy system is not an easy task. Phenomenologically, the usual way to describe the structural state of a glass-forming system is by means of the "fictive temperature", T_f, which was first introduced by Tool.[45] T_f was defined as the temperature at which the value of an intensive property in the supercooled liquid is the one corresponding to the glass. Although from eq 14 a simple relationship between T_f and S_c can be established, other possible relationships have been proposed.[43] On the other hand, it has recently been shown that the temperature dependence of dielectric relaxation times of PVAc in the glassy state[12] are well described by the AG theory only if the contribution of volume change to the total configurational entropy is subtracted.[46] From this result, a different temperature (referred to as isovolume fictive temperature), T_x, is introduced and, therefore, the constant structural state of a glass identified as a constant value of such a temperature.

B. Temperature Dependence of β. The broadening of the α relaxation has usually been interpreted in the framework of different approaches related to the structural disorder characteristic of amorphous systems. In earlier works,[8] the shape of the α relaxation was interpreted to be the result of the superposition of a broad distribution of single (Debye-like) parallel relaxation processes. More recently, the nearly universal characteristics of the α-relaxation have led to the idea that its shape is a consequence of the correlated reorientation of the different relaxing units.[1,3,47] These two pictures, which can be considered to be limiting cases, represent the heterogeneous and homogeneous cases of a general relaxation scheme.[48] In the heterogeneous case each region in the sample behaves following a Debye-like decay, and the non-Debye behavior observed experimentally results from the superposition of different Debye-like processes. On the other hand, in the homogeneous limit all regions in the sample behave in the same way and the non-Debye character arises from the correlation at the level of the relaxing unit involved.

Several extensions of the AG theory to take into account the non-Debye character of the α relaxation have been proposed.[41,49] Matsuoka[41] assumes that the non-Debye character of the α relaxation arises from the presence of cooperatively rearranging regions with different sizes (z^*), thus with different relaxation times; i.e., he considers a heterogeneous approximation. On

the contrary, Ngai[49] assumes that the non-Debye character arises from the correlation among the motions in different cooperatively rearranging regions, which represents a homogeneous scheme. From both models, an increment of β aground 70% when the temperature is varied from T_g to $T_g + 50$ K is deduced. However, the increment of β observed experimentally by us, as well as the ones reported for different polymers in the literature, is rather small (less than 30%). On the other hand, both models predict a nearly Debye behavior at very high temperatures. However, there are only a few systems (not polymer cases) where the value of β approaches unity (Debye-like relaxation) at high temperatures.[22]

Other theoretical approaches in the homogeneous framework predict that β should remain constant at high temperatures;[4,50] i.e., the correlation between relaxing units should not be very affected by temperature changes. For polymers, a limit value for β of about 0.7 is expected in the framework of some models.[50,51] Although this limit is not observed in our measurements, it could be obtained for PVAc and PVME, but the $\beta(T)$ behavior for PH is far from this value.

Since no definitive answer about the correct description of the non-Debye behavior can be obtained from the $\beta(T)$ dependence in the supercooled melt, the way β is affected by the loss of the equilibrium below the glass transition could give insight about this question. Few experimental results concerning the temperature dependence of β in the $T < T_g$ range of glassy polymers are available in the literature.[11,12,13,52,53] Moreover, the results reported show no general trend. However, in spite of the rather scattered values, enthalpic[38] and dielectric[11,12] measurements appear to support our finding that β values around the glass transition are slightly, but systematically, higher than the ones found at equilibrium. Concerning the $\beta(T)$ behavior around T_g, in the framework of a heterogeneous description,[54] a narrowing of the relaxation in the T_g range is expected when one considers that the slower processes freeze at higher temperatures than the faster ones. Moreover, at a given temperature, while the faster processes shift to longer times, before the measurement starts, the slowest processes remain frozen. Thus, in the range where the faster processes have characteristic times shorter than the annealing time involved at the beginning of the experiment, the distribution in the initial stage of the depolarization process would be narrower than the equilibrium one. Moreover, out of equilibrium, below T_g, a continuous decreasing of β is predicted on the basis of the greater temperature coefficients of the larger relaxation times.[41] On the other hand, in the framework of the homogeneous approach no significant change of β when crossing T_g is expected. However, a constant value of β below T_g is predicted.[49]

All the predictions of the heterogeneous scheme, that is, increasing of β with temperature for $T > T_g$, increment of β at T_g, and broadening of the relaxation when the temperature is lowered below T_g, are found experimentally. However, around T_g, the experimental values of β vary in such a small amount that, in a first approximation, one could consider β as a constant around T_g which is predicted by the homogeneous approach. A possible explanation for the experimental $\beta(T)$ behavior is to consider that a distribution of strong correlated processes is responsible for the relaxation shape; i.e., consider a situation intermediate between the homogeneous and the heterogeous limits. With this

picture on mind, we can account for (i) the small increasing of β when through T_g, (ii) the further reduction of β below T_g, and (iii) the weak temperature dependence of the β parameter in the supercooled melt.

A measure of the distribution effects in the relaxation shape (in the parameter β) can be estimated from the increment of β at T_g which is only predicted by the distribution approach. We found that this increment is rather small, which would indicate that the distribution of relaxation processes should be narrow. A possible physical origin for such a distribution can be found in the polydisperse character of the polymers investigated. It is well established that the segmental motion in polymers is affected by the molecular weight, at least in the range of low molecular weights.[5] Since we are dealing with commercial polymers, with a quite high polydispersity (see Table 1), it is not difficult to imagine that the low molecular mass tail of the molecular mass distribution can produce a distribution of relaxation processes. Indeed, recent measurements on nearly monodisperse polymers seem to support this picture since no clear influence of the glass transition on the $\beta(T)$ behavior was detected in this case.[55]

The predictions of the $\beta(T)$ behavior in the supercooled melt are not only dependent on the approach considered but also on the details of the used model. From our results, it is not clear whether the $\beta(T)$ behavior above T_g is related to the presence of a distribution of relaxation processes or not. Despite the fact that $\beta(T)$ is nearly constant in the T range above T_g for PH, it is for this polymer that we obtain the highest increment at T_g. On the contrary, for PVAc and PVME, where a clear temperature dependence of β is observed, the increment at T_g is not so pronounced. The main structural difference of PH with respect to the other two polymers is that PH is a main polymer, whereas PVAc and PVME have the polar unit in the side group. Moreover, PH has hydrogen-bonding interactions among the chain which can be detected by means of infrared spectroscopy. Whether these structural differences can be related to the $\beta(T)$ behavior above T_g or not is a question that still remains unclear.

V. Conclusions

We have reported on the effect of the experimental liquid–glass transition on the dielectric relaxation of three amorphous polymers. It has been established that, by means of the time domain method, it is possible to characterize the dynamics in a predetermined glassy state. The state characterized is not the one obtained by a continuous cooling down to the temperature of measurement but the one with a lower enthalpy. Once the enthalpy recovery behavior is known, the adequate selection of the experimental conditions allows one to characterize the same state at all temperatures below T_g.

It was found that the relaxation behavior can be well described by the KWW relaxation function above and below T_g, i.e., in the supercooled melt and in the glassy state. We observed that the KWW parameters characteristic of both the rate and the shape of the relaxation process are, to some extent, affected by the liquid–glass transition. The temperature dependence of the characteristic time scale shows a clear crossover from VF behavior toward a Arrhenius behavior in the liquid–glass transition range. This complex $\tau(T)$ behavior, which extends over 10 decades in time scale, can be fully accounted for in the AG theory framework if a slow change of $S_c(T)$ in the glassy state is allowed. On the other hand, when the system falls out of equilibrium, the KWW shape parameter β seems to be slightly higher than the one corresponding to the supercooled liquid. This effect has been interpreted to be produced by the presence of a distribution of relaxation processes. However, it seems that the relaxation shape is not mainly determined by this distribution. This result led us to propose that a distribution of strongly correlated (non-Debye in nature) relaxation processes is underlying the α relaxation. A careful test of this interpretation will be reported in the near future.[55]

References and Notes

(1) *Relaxation in Complex Systems*; Ngai, K. L., Wright, G. R., Eds.; North-Holland: Amsterdam, The Netherlands, 1991.
(2) *Basic Features of the Glassy State*; Colmenero, J., Alegría, A., Eds.; World Scientific: Singapore, 1990.
(3) *Dynamics of Disordered Materials II*; Dianoux, A. J., Petry, W., Richter, D., Eds.; Elsevier Science Publishers: Amsterdam, The Netherlands, 1993.
(4) Götze, W. In *Liquids, Freezing and the Glass-Transition*; Les Houches Summer School, Course LI, July 1989; Hansen, J. P., Levesque, D., Zinn-Justin, J. Eds.; North-Holland: Amsterdam, The Netherlands, 1991; p 289.
(5) Ferry, J. D. *Viscoelastic Properties of Solid Polymers*; John Wiley and Sons: New York, 1979.
(6) Gibbs, J. H.; Di Marzio, E. A. *J. Chem. Phys.* **1958**, *28*, 373.
(7) Stillinger, F. H. *J. Chem. Phys.* **1988**, *88*, 7818.
(8) McCrum, N. G.; Read, B. E.; Williams, G. *Anelastic and Dielectric Effects in Polymeric Solids*; Wiley: London, 1967.
(9) Kovacs, A. J. *Fortschr. Hochpolym.-Forsch.* **1963**, *3*, 394.
(10) Struik, L. C. E. *Physical Aging in Amorphous Polymers and Others Materials*; Elsevier: Amsterdam, The Netherlands, 1978.
(11) Alegría, A.; Guerrica-Echevarria, E.; Tellería, I.; Colmenero, J. *Phys. Rev. B* **1993**, *47*, 14857.
(12) Schlosser, E.; Schönhals, A. *Polymer* **1991**, *32*, 2135.
(13) Hodge, I. M. *Macromolecules* **1987**, *20*, 2897.
(14) Lee, H. H.; McGarry, F. J. *Polymer* **1993**, *34*, 4267. Monserrat, S. *J. Polym. Sci. B* **1994**, *32*, 509.
(15) Alegría, A.; Guerrica-Echevarria, E.; Goitiandia, L.; Tellería, I.; Colmenero, J., in preparation.
(16) Adams, G.; Gibbs, J. H. *J. Chem. Phys.* **1958**, *43*, 139.
(17) Di Marzio, E. A.; Dowell, F. *J. Appl. Phys.* **1979**, *50*, 6061.
(18) Böttcher, C. J. F. *Theory of Electric Polarization*; Elsevier Scientific: Amsterdam, The Netherlands, 1973.
(19) Alvarez, F.; Alegría, A.; Colmenero, J. *Phys. Rev. B* **1991**, *44*, 7306.
(20) Alvarez, F.; Alegría, A.; Colmenero, J. *Phys. Rev. B* **1993**, *47*, 125.
(21) Nozaki, R.; Mashimo, S. *J. Chem. Phys.* **1987**, *57*, 2271.
(22) Schönhals, A.; F. Kremer, F.; Schlosser, E. *Phys. Rev. Lett.* **1991**, *67*, 999.
(23) Sassabe, H.; Moynihan, C. T. *J. Polym. Sci., Polym. Phys.* **1978**, *16*, 1447.
(24) Zetsche, A.; Kremer, F.; Jung, W.; Schulze, H. *Polymer* **1989**, *31*, 1833.
(25) Colmenero, J.; Alegría, A.; Alberdi, J. M.; Alvarez, F.; Frick, B. *Phys. Rev. B* **1991**, *44*, 7321.
(26) Angell, C. A. *J. Non-Cryst. Solids* **1991**, *131–133*, 13.
(27) Alegría, A.; Goitiandia, L.; Tellería, I.; Colmenero, J. *J. Non-Cryst. Solids* **1991**, *131–133*, 457.
(28) Alegría, A.; Guerrica-Echevarria, E.; Tellería, I.; Colmenero *Trends in Non-Crystalline Solids*; Conde, A.; Conde, C. F., Millan, M., Eds.; World Scientific: Singapore, 1992; p 301.
(29) Cohen, M. H.; Grest, G. S. *Phys. Rev. B* **1979**, *20*, 1077.
(30) Goldstein, P.; del Castillo, L. F.; García-Colín, L. S. *Macromolecules* **1993**, *26*, 655.
(31) Doolittle, A. K. *J. Appl. Phys.* **1951**, *22*, 1471.

(32) Cohen, M. H.; Turnbull, D. *J. Chem. Phys.* **1959**, *31*, 1164.
(33) Robertson, R. E.; Simha, R.; Curro, J. G. *Macromolecules* **1988**, *21*, 3216.
(34) Bondi, A. A. *Physical Properties of Molecular Crystals, Liquids, and Crystals*; John Wiley & Sons: New York, 1960. Lee, W. M. *Polym. Eng. Sci.* **1980**, *20*, 65.
(35) Angell, C. A.; Bressel, R. D. *J. Phys. Chem.* **1972**, *76*, 3244.
(36) Goldstein, M. *J. Chem. Phys.* **1965**, *43*, 139.
(37) Di Marzio, E. A.; Dowell, F. *J. Appl. Phys.* **1979**, *50*, 6061.
(38) Hodge, I. M. *J. Non-Cryst. Solids* **1994**, *169*, 211.
(39) Flory, P. J. *Statistical Mechanics of Chain Molecules*; Hanse Publishers Press: New York, 1989; p 247.
(40) Winderlich, B.; Baur, H. *Adv. Polym. Sci.* **1970**, *7*, 151.
(41) Matsuoka, S.; Quan, X. *Macromolecules* **1991**, *24*, 2770.
(42) Mathot, V. B. F. *Polymer* **1984**, *25*, 579.
(43) Hodge, I. M. *Macromolecules* **1986**, *19*, 936.
(44) Scherer, G. W. *J. Am. Ceram. Soc.* **1984**, *67*, 504.
(45) Tool, A. Q. *J. Am. Ceram. Soc.* **1946**, *28*, 240.
(46) Spathis, G. *Polymer* **1994**, *35*, 791.

(47) Adachi, K. *Macromolecules* **1990**, *23*, 1816.
(48) Richert, R.; Blumen, A. *Disorder Effects on Relaxation Processes*; Richert, R., Blumen, A., Eds.; Springer-Verlag: Berlin, 1994; p 1.
(49) Ngai, K. L. Reference 1, p 80.
(50) Helfand, E.; Wasserman, Z. R.; Weber, T. A. *J. Chem. Phys.* **1979**, *70*, 2016.
(51) Schönhals, A.; Schlosser, E. *Colloid. Polym. Sci.* **1989**, *267*, 125.
(52) Alegría, A.; Goitiandía, L.; Tellería, I.; Colmenero, J. *J. Non-Cryst. Solids* **1991**, *131–133*, 457.
(53) Ngai, K. L. In *Non-Debye Relaxation in Condensed Matter*; Ramakrishnan, T. V., Raj Lakshmi, M., Eds.; World Scientific: Singapore 1987; p 23–191 and references cited therein.
(54) Moynihan, C. T.; Schroeder, J. *J. Non-Cryst. Solids* **1993**, *160*, 52.
(55) Hofmann, A.; Alegría, A.; Colmenero, J., to be published.

MA941296U